Effects of Water-soluble Organic Carbon on Aerosol pH

Michael A. Battaglia, Jr.[1], Rodney J. Weber[2], Athanasios Nenes[2,3,4], Christopher J. Hennigan[1*]

[1] Department of Chemical, Biochemical and Environmental Engineering, University of Maryland, Baltimore County, Baltimore, MD 21250, USA

[2] School of Earth and Atmospheric Sciences, Georgia Institute of Technology, Atlanta, GA 30332, USA

[3] Institute for Chemical Engineering Sciences, Foundation for Research and Technology – Hellas, Patras, 26504, Greece

[4] Laboratory of Atmospheric Processes and their Impacts, School of Architecture, Civil and Environmental Engineering, Ecole Polytechnique Fédérale de Lausanne, CH-1015, Lausanne, Switzerland

[*]To whom correspondence should be addressed: email hennigan@umbc.edu; phone: (410) 455-3515

Abstract

Water soluble organic carbon (WSOC) is a ubiquitous and significant fraction of fine particulate matter. Despite advances in aerosol thermodynamic equilibrium models, there is limited understanding on the comprehensive impacts of WSOC on aerosol acidity (pH). We address this limitation by studying submicron aerosol that represent the two extremes in acidity levels found in the atmosphere: strongly acidic aerosol from Baltimore, MD, and weakly acidic conditions characteristic of Beijing, China. These cases are then used to construct mixed inorganic/organic single-phase aqueous particles, and thermodynamically analyzed by the E-AIM and ISORROPIA models in combination with activity coefficient model AIOMFAC to evaluate the effects of WSOC on the H^+ ion activity coefficients (γ_{H+}) and activity (pH). We find that addition of organic acids and non-acid organic species concurrently increases γ_{H+} and aerosol liquid water. Under the highly acidic conditions typical of the eastern U.S. (inorganic-only pH ~1), these effects mostly offset each other, giving pH changes of < 0.5 pH units even at organic aerosol dry mass fractions in excess of 60%. Under conditions with weaker acidity typical of Beijing (inorganic-only pH ~4.5), the non-acidic WSOC compounds had similarly minor effects on aerosol pH, but organic acids imparted the largest changes in pH compared to the inorganic-

only simulations. Organic acids affect pH in the order of their pKa values (oxalic acid > malonic acid > glutaric acid). Although the inorganic-only pH was above the pK_a value of all three organic acids investigated, pH changes in excess of 1 pH unit were only observed at unrealistic organic acid levels (aerosol organic acid concentrations > 35 μg m^{-3}) in Beijing. The model simulations were run at 70%, 80%, and 90% relative humidity (RH) levels and the effect of WSOC was inversely related to RH. At 90% RH, WSOC altered aerosol pH by up to ~0.2 pH units, though the effect was up to ~0.6 pH units at 70% RH. The somewhat offsetting nature of these effects suggests that aerosol pH is sufficiently constrained by the inorganic constituents alone under conditions where liquid-liquid phase separation is not anticipated to occur.

1. Introduction

The acidity of atmospheric particles plays a critical role in many physicochemical processes. Some of these processes include sulfur oxidation and halogen chemistry, with important implications for the formation of sulfates (Chameides, 1984) ; the oxidation of volatile organic compounds (VOCs), and ozone formation in marine environments (Keene et al., 1998); the gas-particle partitioning of many semi-volatile species (Ahrens et al., 2012; Keene et al., 2004); and, enhancements to secondary organic aerosol (SOA) formation (Hallquist et al., 2009). The inorganic salt constituents in atmospheric particles, such as ammonium sulfate ($(NH_4)_2SO_4$) and ammonium bisulfate (NH_4HSO_4), contribute to particle acidity and water content, with effects on aerosol radiative forcing (Seinfeld and Pandis, 2016). In addition to the physicochemical effects within particles, their bulk acidity can affect health, both of environmental ecosystems and the human populations therein either directly (Gwynn et al., 2000; Peters et al., 1996; Schindler, 1988; Spengler et al., 1996; Fang et al., 2017; Johnson et al., 2008), or by their effects on nutrient deposition (Myriokefalitakis et al., 2016; Myriokefalitakis et al., 2018; Kanakidou et al., 2016; Nenes et al., 2011).

pH, the parameter serving to define and describe the acidity of aqueous solutions, often has no direct correlation with proxy measurement methods such as aerosol strong acidity (H^+ contributed by strong acids that dissociated completely at any pH level) or aerosol total acidity (dissociated H^+ and undissociated H^+ bound to weak acids) (Hennigan et al., 2015; Song et al., 2018b). The most accurate predictions of aerosol pH come from aerosol thermodynamic equilibrium models constrained by both aerosol and gas-phase measurements (i.e., "forward mode" calculations), or from the measured gas-particle partitioning of semi-volatile species, including ammonia, nitric acid, or oxalic acid, which provide direct insight to the pH (Hennigan et al., 2015). Both approaches utilize aerosol and gas-phase composition measurements, along with the temperature and relative humidity, to obtain aerosol pH values. Consistent pH values are obtained when the assumptions about aerosol mixing and equilibrium are met (Guo et al., 2018a; Guo et al., 2018b).

Different aerosol thermodynamic equilibrium models have been developed through the years, each with a unique sets of assumptions, simplifications and approach to obtain the composition at thermodynamic equilibrium. The Extended Aerosol Inorganics Model (E-AIM, http://www.aim.env.uea.ac.uk/aim/aim.php) (Wexler and Clegg, 2002; Friese and Ebel, 2010) and the ISORROPIA-II model (Greek for 'equilibrium,' http://isorropia.eas.gatech.edu) (Fountoukis and Nenes, 2007) are widely used to calculate aerosol pH for atmospheric and experimental particle distributions (Guo et al., 2017; Guo et al., 2016; Guo et al., 2015; Wang et al., 2016). The Aerosol Inorganics-Organics Mixtures Functional groups Activity Coefficient (AIOMFAC) model (http://www.aiomfac.caltech.edu/model.html) offers the most extensive treatment of organic-inorganic interactions (Zuend et al., 2008; Zuend et al., 2011) of models to date, but is primarily an activity coefficient model that does not solve full thermodynamic

78 equilibrium calculations or phase partitioning as E-AIM and ISORROPIA do. At present, E-
79 AIM, ISORROPIA, and AIOMFAC are widely used for atmospheric applications due to their
80 demonstrated predictive capabilities and their accessibility: they are freely available online, and
81 include resources and user guides to facilitate their application and use.

82 One key difference among the models is their treatment of organics. ISORROPIA does not
83 include organic species. E-AIM functions similarly to ISORROPIA when considering inorganic
84 species, but in addition offers a limited library of organic acids (included by UNIFAC methods
85 or fitted activity equations). AIOMFAC offers wide support for organic components, but is an
86 activity coefficient model that does not solve the equilibrium partitioning calculations for which
87 the other models were designed. While AIOMFAC has been used in combination with
88 thermodynamic equilibrium models such as ISORROPIA-II (Pye et al., 2018), these are custom
89 modifications to the models, and not reflected in the online versions used in this study. These
90 models, and most others, do not treat organics in a way that is comprehensive (that is,
91 simultaneous consideration of activity coefficient calculations and thermodynamic equilibrium
92 calculations). However, these simplified thermodynamic models do seem to capture the
93 partitioning of inorganic species well, even when organic components are present in large
94 quantities, which indicates that pH should be captured well (Guo et al., 2018a). An additional
95 consideration between the models is their treatment of organic acids. E-AIM offers support for
96 limited (n = 8) organic acid species, and treats the dissociation equilibrium of organic acids. In
97 contrast, AIOMFAC treats organic acids as non-dissociating, a model difference that is discussed
98 in detail below. Note that the ion dissociation equilibria of inorganic species (such as HSO_4^-
99 /SO_4^{2-}) are explicitly considered in the equilibrium calculates of all three models employed in
100 this study.

The effects of WSOC on aerosol pH come through two primary means: dilution of the aqueous phase by aerosol liquid water associated with the organic fraction (W_o); and changes to the hydrogen ion activity coefficient and thus hydrogen activity in solution (γ_{H+} and a_{H+}, respectively). The total contribution of organics to aerosol water can be as much as 30-50% of total fine particle aerosol water in the polluted Beijing winter haze events (Tan et al., 2018; Huang et al., 2014), 40-50% in the southeast United States (Nah et al., 2018; Guo et al., 2015), and the eastern Mediterranean (Bougiatioti et al., 2016). The effects of organics (soluble and insoluble) on aerosol pH under conditions of liquid-liquid phase separation (LLPS) are more complex. Free H^+ ion is predicted to have increased association with SO_4^{2-} to form HSO_4^- when organic compounds are in the same phase as inorganic ions, resulting in a 0.1 pH unit increase in aerosol pH (Pye et al., 2018). The isolation of the organic components in a separate phase (LLPS condition) also alters the partitioning behavior of NH_3, a critical component that contributes to aerosol pH. The inclusion, or lack thereof, of organic compounds was predicted to have a greater effect on NH_3 partitioning behavior than the inclusion, or lack thereof, of nonvolatile cations, nitrate, and chloride (Guo et al., 2018a). In addition to these effects, AIOMFAC predicts that any organic presence in the same phase with inorganic constituents drives free H^+ to increased association with sulfate to form bisulfate, a compound predicted to be more miscible with organics than H^+ and small cations. AIOMFAC was used to show that the organic phase of liquid-liquid phase separated particles still contains a significant amount of inorganics, affecting the partitioning medium by inclusion of the inorganic ions and their associated water, lowering the mole fraction and activity of organics, and shifting the gas-particle partitioning of organic compounds with O:C > 0.6 (Pye et al., 2018). In the case where multiple phases do exist, there is anticipated to be a primarily-organic (PO) and primarily-

inorganic (PI) phase, each of which contains H^+ in equilibrium with the other phase. In cases where the vast majority of inorganics are partitioned to the PI phase, the pH is not anticipated to change drastically, as H^+ is also required to be in equilibrium with the other phases, which may explain the results of (Pye et al., 2018). In the case of phase separation where the PO phase contains considerable amounts of inorganic species, there exists the possibility of a PI phase with substantially-altered H^+ activity, and therefore, the potential for substantially-altered aerosol pH (*eg.* (Dallemagne et al., 2016). The present study avoids such complexity and instead considers mixed organic-inorganic particles present in a single aqueous phase.

Aerosol pH can also be directly affected by organic acids, whose dissociation produces H^+ ions in the particle aqueous phase. Carboxylic acids represent a highly abundant moiety in atmospheric OA (Yatavelli et al., 2015; Kawamura and Bikkina, 2016; Nah et al., 2018). Although these atmospheric organic acids are typically weaker acids with higher pK_a values than common inorganic acids (H_2SO_4 and HNO_3), they may contribute to particle acidity in some environments (Trebs et al., 2005). However, this effect is not present in all environments and is constrained to situations where the pH is in the range of the pK_a of the acid in question (Nah et al., 2018; Song et al., 2018b). As both organic acids and non-acid organic species are expected to be present, there are competing effects within the particle: dilution by the water fraction associated with organic constituents, direct acidification by the dissolution of organic acids, and the change in γ_{H+} by interactions with the additional species in solution.

Oxalic acid (measured as the oxalate ion) is often the most abundant carboxylic acid in atmospheric aerosols (Bikkina et al., 2015). Several studies utilized E-AIM Model IV to evaluate the effect of oxalic acid on particle acidity (Vasilakos et al., 2018; Song et al., 2018b). With inorganics similar in composition to that of Baltimore, conditions applied in this study, an

increase of 25-50% of oxalic acid compared to the base case had an insignificant effect on aerosol pH when only one liquid phase was present. Pye et al. (2018) utilized data from the Southern Oxidant and Aerosol Study (SOAS) in ISORROPIA and AIOMFAC to investigate the gas-particle partitioning of ammonia, water, and organic compounds, and how liquid-liquid phase separation (LLPS) in particles can affect aerosol pH, predicting a 0.7 pH unit increase when the organic fraction and its diluting effect was considered. Generally, aerosol processes are not affected by a pH change of this magnitude, except in the regions on the thermodynamic sigmoid curves of semi-volatile species where partitioning is shown to vary greatly for small changes in pH (Nah et al., 2018; Guo et al., 2018b).

In this work, we explore the effects of WSOC on aerosol pH in a systematic way by utilizing inorganic data to construct combinations of single, aqueous phase particulate compositions, and utilizing aerosol thermodynamic models to investigate the effects of different WSOC species and concentrations on γ_{H+} and a_{H+}.

2. Methods

Data

Inorganic and meteorological data used for this study were reported in prior work. Briefly, data from Baltimore, MD were taken from (Battaglia et al., 2017), and include speciated inorganic $PM_{2.5}$ concentrations, meteorological data, and gas-phase NH_3 measurements. The data used as thermodynamic model inputs are summertime (July) averages based on 3- or 5-years of monitoring. All model inputs and outputs are available at https://knb.ecoinformatics.org/ (doi: TBD –upon acceptance).

Aerosol inorganic composition, gas-phase NH_3 measurements, and meteorological parameters were obtained during a study of winter haze formation in Beijing, China in 2015 (Wang et al., 2016). These data represent a contrast with Baltimore due to different source contributions, differences in NH_3 concentrations, T, RH, and inorganic aerosol levels. The inorganic $PM_{2.5}$ concentrations, and averaged seasonal T and RH, along with NH_3 gas concentration values were obtained as model-ready inputs of the Beijing winter haze data from (Guo et al., 2018b), based on supplemental information from (Wang et al., 2016).

General Approach

The general approach to this study was to utilize the inorganic PM and NH_3 data described above, in combination with various additional WSOC constituents, as inputs to aerosol thermodynamic equilibrium models to investigate the effects on model-predicted aerosol pH and γ_{H+}. Inorganic data were modeled in either E-AIM IV or ISORROPIA-II to obtain equilibrium concentrations of aerosol liquid water (ALW) along with all inorganic aerosol ionic species. Organic constituents were then added to this invariant inorganic matrix (assuming the added organic mass was at equilibrium), at identical T and RH, and the resulting particle compositions were modeled in AIOMFAC to obtain aerosol H^+ ion activity (a_{H+} and γ_{H+}), and thus aerosol pH. The average inorganic composition, gas-phase NH_3, and meteorological conditions were held approximately constant for each location, while WSOC composition and concentrations were systematically varied. A matrix was constructed to examine multiple combinations of the selected organic component composition levels (factorial design), and their effects evaluated on the basis of organic-to-inorganic ratio (OIR) or organic mass fraction, both computed on a dry particle basis. This full factorial design consists of three factors for each acid or non-acid condition (the identity of each species), each with discrete possible values (air concentrations in

μg m^{-3}), where the experiment incorporates all possible combinations of these values across all factors (Keppel, 1991). For each location, this resulted in a total of 7986 model simulations in total, with 1331 simulations run for both cases of organic compounds selected, and at each of three distinct RH level, as described below. A summary of the models run for each location is shown in **Table 1**. The RH in all simulations was fixed at either ~70%, ~80%, or ~90%, with inorganic system inputs calculated and invariant at each RH level based on the initial input data from either Baltimore or Beijing to ensure deliquescence of inorganic aerosol particles, to understand the sensitivity of the model-predicted aerosol pH to changes in RH (ALW), and to avoid liquid-liquid phase separation as a potential cause of organic-influenced aerosol pH changes (Pye et al., 2018). For all of the results presented in this analysis, aerosol pH was computed as the negative base-ten logarithm of the hydrogen ion activity taken from the E-AIM or AIOMFAC output ($pH = -\log_{10} a_{H+}$) on a molality basis.

Organic Constituents

Water-soluble organic compounds were selected by broadly classifying them as organic acids or non-acid organics. Within each category, three individual species were selected based on their detection in atmospheric particles and their availability in the predefined list of AIOMFAC organic species available on the AIOMFAC web interface, or the ability to reasonably construct them using the functional groups approach of AIOMFAC. In addition, non-acid organics were selected from three different primary moiety groups from among the AIOMFAC standard species. Oxalic acid ($C_2H_2O_4$ $pK_{a1} = 1.23$, $pK_{a2} = 4.19$) (Lide 1994) , glutaric acid ($C_5H_8O_4$, $pK_{a1} = 4.31$, $pK_{a2} = 5.41$) (Lide, 1994), and malonic acid ($C_3H_3O_4$, $pK_{a1} = 2.83$, $pK_{a2} = 5.69$) (Lide, 1994) were selected as the three dicarboxylic acid species. Levoglucosan ($C_6H_{10}O_5$), tetrahydrofuran ($(CH_2)_4O$), and 2-methyltetrol (1-methylbutane-1,2,3,4-tetrol, $C_5H_{12}O_4$), three

organic species observed in ambient aerosols, were selected as the non-acid WSOC species. Concentration levels were not constrained by observations, but were instead selected to achieve similar organic to inorganic mass ratios for each of the two geographic regions being considered. For Beijing, typical organic mass fractions can be on the order of 50-70% of total aerosol mass (Zhou et al., 2018), and 20-60% of total aerosol mass for continental mid-latitude locations like Baltimore (Carlton et al., 2009). For each geographic region, 11 different concentrations were chosen for each WSOC compound (0-4 μg m^{-3} for Baltimore; 0-40 μg m^{-3} for Beijing), and combined in factorial fashion: each organic acid concentration level combination of the three organic acids were examined in combination with every other level of the remaining two, and vice-versa for the non-acid organic species. Combinations of organic acids and non-acid organic species were not explicitly considered here; only combinations of organic acids with organic acids, or combinations of non-acids with non-acids were examined experimentally. All model inputs and outputs are available at https://knb.ecoinformatics.org/ (doi: TBD –upon acceptance).

Thermodynamic Model Input Configuration and Equilibrium Model Evaluations

E-AIM Model IV provides thermodynamic equilibrium modeling of the H^+-NH_4^+-Na^+-SO_4^{2-}-NO_3^--Cl^--H_2O system at temperatures from 263.15 K to 330 K for subsaturated systems that contain NH_4^+ and Cl^-, or Na^+ in combination with other ions (Friese and Ebel, 2010). Data for Baltimore and Beijing were formatted for E-AIM input in the following ways: average inorganic species concentrations (μg m^{-3}) were converted to mol m^{-3}; the average daily temperature for the same period was used as the temperature input; the relative humidity of the system was fixed (at 70%, 80%, or 90%) both to ensure the inorganic system was in a deliquesced state and because of the RH restrictions (subsaturated solution requirements, RH > 0.6) on E-AIM Model IV inputs. In addition to fixing system RH at 70%, 80%, or 90%, the aerosol metastable (solid

237 precipitate formation disabled) mode was enforced on the model by disabling the formation of all
238 solids in the model input matrix, according to the analysis and recommendation of Guo et al.
239 (2018b; 2015). Crustal species (Ca^{2+}, Mg^{2+}, K^{+}) not supported by the model were not
240 considered, and the persistent cation deficiency was corrected by the addition of H^{+} to the system
241 to ensure electroneutrality. The amount of H^{+} added was a not-insignificant amount, comprising
242 approximately 65% of the amount of NH_4^{+} included in the model for Baltimore, but makes sense
243 given the expected acidic nature of eastern US, sulfate-rich aerosols (Weber et al., 2016). For
244 Beijing, a persistent anion deficiency was addressed by addition of OH^{-} to the system to ensure
245 electroneutrality. The amount of OH^{-} added to the system for the Beijing case was one order of
246 magnitude lower than the cation species, but on the same order of magnitude and 4-7 times lower
247 than any other anion except Cl^{-}.

248 E-AIM offers support for certain organic acid species. For the Baltimore and Beijing
249 simulations, the organic acid species were added directly to the E-AIM model inputs. In the case
250 of organic acid model runs, factorial combinations of the organic acid species at 0.0, 0.01. 0.02,
251 0.04, 0.08, 0.16, 0.32, 0.5, 1, 2, and 4 μg m^{-3} (Baltimore) and 0.0, 1, 2, 5, 10, 15, 20, 25, 30, 35,
252 and 40 μg m^{-3} (Beijing) and were converted to mol m^{-3} input. Formation of organic solids was
253 also disabled as part of the metastable equilibrium condition. For the non-acid organics, the
254 addition of the selected species to the E-AIM equilibrium calculation was not possible, and the
255 model was run with the inorganic constituents only. E-AIM provides output of the aqueous
256 species mole fractions and mole fraction-based activity coefficients; this mole fraction-based
257 aerosol pH was converted to a molality-based aerosol pH utilizing known thermodynamic
258 relations (Robinson and Stokes, 1965; Jia et al., 2018).

259 **ISORROPIA-II Model Input Configuration and Equilibrium Model Evaluations**

ISORROPIA-II provides thermodynamic equilibrium modeling for the H^+-NH_4^+-Na^+-SO_4^{2-}-NO_3^--Cl^--Ca^{2+}-Mg^{2+}-K^+- H_2O across a wide range of temperature and RH values without limitation based on the input composition (Fountoukis and Nenes, 2007). Data for Beijing were already formatted for use in ISORROPIA-II as described above (Guo et al., 2018b). The formation of solids in the model was disabled (leading to potential supersaturated aerosols, metastable mode operation), based on the justifications in previous studies (Guo et al., 2015; Guo et al., 2018b) and to maintain consistency with the E-AIM model conditions. An initial model run was performed to verify that identical model outputs were obtained using the inputs of Guo et al. (2018b). For the purposes of this investigation, the RH value was changed from the Beijing average ambient value of 56% to 70%, 80%, or 90%, consistent with the model input for the Baltimore data for the same reasons discussed above. The Beijing average ambient temperature of 274.05 K was used in the Beijing inorganic model calculations with the three RH values.

AIOMFAC Model Input Configuration and Equilibrium Model Evaluations

E-AIM was utilized to determine the equilibrium composition of the inorganic aerosol, including the NH_3 phase partitioning and the aerosol liquid water content. Outputs from E-AIM were then used as inputs into AIOMFAC to characterize the organic effects on aerosol H^+ activity, and γ_{H+} (**Figure 1**). The E-AIM outputs (AIOMFAC inputs) were also checked for consistency with ISORROPIA to ensure that the applied model assumptions (H^+ and OH^- as balancing species to achieve electroneutrality) provided reasonable results.

The particle-phase outputs from the E-AIM model runs were used as inputs to AIOMFAC; however, this required significant adjustments to the format to fit the AIOMFAC model. AIOMFAC requires inorganic species inputs to be entered as ionic *pairs* (whole molecular species entered as a cation and anion pair) in order to guarantee electroneutrality. Therefore, the

ionic species outputs of E-AIM were converted to molecular species inputs by assigning pairs, and then performing a stoichiometric balance until all ions were accounted for (*i.e.* E-AIM H^+ and SO_4^{2-} being combined in stoichiometric fashion as H_2SO_4 with corresponding reductions in the 'pool' of E-AIM H^+ and SO_4^{2-}). In the Baltimore case for the pure inorganic input (all organic species modeled at 0.0 μg m^{-3} concentration), E-AIM Model IV provided particle-phase output for the following ions: H^+, NH_4^+, Na^+, HSO_4^-, SO_4^{2-}, NO_3^-, and OH^-. In order to format these concentrations for AIOMFAC-specific inputs (that is, to compute the necessary mole fraction format of molecular species in the aerosol), the ions were assigned in the following ways. First, all SO_4^{2-} was associated with H^+ for the H_2SO_4 pair in AIOMFAC. All NO_3^- was associated with Na^+ for the $NaNO_3$ pair. Remaining Na^+ was associated with SO_4^{2-}, then NH_4^+ with HSO_4^- and remaining NH_4^+ with the remaining SO_4^-. This allocation process proceeded similarly for the Beijing data. The selected species and order of allocation of the ionic species appears to be dependent solely on the user, and *a priori* knowledge of which molecular species are likely to exist in the aerosol particle as the dissociated ionic species. The selection of species is unlikely to affect model outcomes, as this is simply a way to account for the ionic species present in the AIOMFAC model inputs, which require matched cation-anion pairs, and are expected to be fully-dissociated in the aqueous phase during model evaluation. The end result is a mixture of inorganic molecular species containing the full concentration values generated by E-AIM assumed to be dissociated within the aerosol where each functional group can contribute to species activity based on the AIOMFAC model paradigm; assignment of molecular species pairings is performed only on the basis of formatting specifically for the AIOMFAC model. The inorganic inputs used in the AIOMFAC models for both Baltimore and Beijing simulations are given in **Table 2**.

306 An additional key step in formatting the E-AIM output for input to AIOMFAC is in the model
307 treatment of the water associated with organic constituents, W_o. E-AIM provided output of W_o
308 as a part of the total aerosol liquid water (ALW; $W_i + W_o$) for the organic acid simulations, but
309 provides no estimate of W_o for the non-acid simulations. RH is not an input to the AIOMFAC
310 model runs. Rather, AIOMFAC requires the input of all species (inorganic and organic) in mole
311 fractions, and assumes the difference between the total inputs and unity is contributed by water,
312 the water activity of which is equal to the ambient relative humidity. Therefore, accounting for
313 the water contributed by the organic species was an additional step in formatting the E-AIM
314 outputs for AIOMFAC input as described below.

315 For two of the four cases (Baltimore and Beijing inorganics plus non-acid organics), W_o was
316 added to the system by the following process, a flow diagram of which is shown in **Figure 1**.
317 For the first 11 points of the factorial design (representing the addition of only the first organic
318 constituent at each concentration level) and the final 11 points of the factorial design
319 (representing the 11 highest organic addition points, including the addition of all three organic
320 species at their maximum selected concentration), total system moles were varied manually by
321 increasing the inorganic model-predicted moles of aerosol water. AIOMFAC inputs (as mole
322 fractions) were calculated using this adjusted total mole value. The 22 manually-adjusted points
323 were modeled in AIOMFAC. If the option for liquid water is selected (as it was in all of our
324 simulations), AIOMFAC assumes that water makes up the difference between the mole or mass
325 fraction of all inputs summed together and unity. To achieve consistency with the inorganic
326 model results, the total moles of the system were manually adjusted until the RH output
327 generated by the AIOMFAC model was within ~5% of the RH value fixed for the inorganic
328 systems. Once this close fit was achieved for the 22 selected points, they were used to generate

polynomial fits of the total moles added to the system as W_o versus total organic mass (regardless of species). These polynomial fits were then applied to all model points to adjust the total system moles through the addition of liquid water associated with organic mass, resulting in AIOMFAC-predicted RH values within 5% of the E-AIM RH values of 70%, 80%, or 90%. This method of accounting for W_o is a strictly mathematical construct, and does not reflect the use of a species-dependent organic hygroscopicity parameter, which would have been prohibitive to apply for each point across all cases and RH levels. Additionally, following the introduction of the adjusted W_o to the system, the gas-phase was not allowed to re-equilibrate to the new water content contributed by the organic species. This provides a conservative (high) constraint on the effect of W_o (Guo et al., 2015).

Evaluation of LLPS and Accommodations for LLPS Scenarios

The O:C ratio is a key factor that determines whether LLPS occurs in organic-containing particles (Song et al., 2018a; Freedman, 2017). We followed the parameterization found experimentally by Bertram et al. (2011) to evaluate the presence of LLPS in our simulations. This method uses the overall mixture O:C ratio to determine the separation RH of the mixture. If the modeled (in this case, specified/enforced) system RH is lower than the parameterized separation RH (RH_{LLPS}), LLPS is likely to occur. This was performed for each of the non-acid mixtures for both Baltimore and Beijing data to verify the claim that LLPS was not anticipated to occur. For cases where the parameterized RH_{LLPS} was higher than the predicted system RH, LLPS was anticipated to occur, and the point was flagged and excluded from further analysis. Out of 1331 simulations, Baltimore had 55% (n = 732), 70% (n = 932), and 75% (n = 998) simulations that met the non-LLPS criteria at 70%, 80%, and 90% RH respectively. Beijing had 85% (n = 1131), 89% (n = 1185), and 93% (n = 1238) of simulations meet the non-LLPS

conditions at 70%, 80%, and 90% RH respectively. Experimental work by (You et al., 2013) indicates that glutaric acid, malonic acid, oxalic acid, or their mixtures do not undergo LLPS at any of the RHs investigated.

3. Results and Discussion

Effects of WSOC on Aerosol γ_{H+}

AIOMFAC-predicted aerosol pH and γ_{H+} versus the organic dry mass fraction (total mass of organics/mass inorganics, excluding ALW), along with aerosol liquid water used in the model evaluations for the non-acid species runs in Baltimore and Beijing at al RH levels, are shown in Figures 2 and 3. For the case of non-acid WSOC compounds at 80% RH (Figs. 2d and 3d), ALW increases from 4.7×10^{-9} L m^{-3} to 9.7×10^{-9} L m^{-3} and from 9.6×10^{-8} L m^{-3} to 1.8×10^{-7} L m^{-3} for Baltimore and Beijing, respectively, as the organic mass fraction increases. Similar trends follow for the 70% and 90% RH scenarios in both cities. This behavior makes sense, because the inorganic species concentrations and RH were fixed, so adding increasing levels of water-soluble organics increases the ALW. Increasing the organic dry mass fraction increases the value of γ_{H+}, from initial values of 0.10 and 0.16 (80% RH) for Baltimore and Beijing under inorganic-only conditions, to 2.4 for Baltimore (Fig. 2d) and 1.6 for Beijing (Fig. 3d). The higher absolute ALW levels in the Beijing simulations are due to the significantly higher inorganic and organic aerosol loadings.

The results follow for the additional RH values studied. For the case of non-acid organics at 70% RH (Figs. 2 and 3) increasing the organic dry mass fraction increases the value of γ_{H+}, from initial values of 0.11 and 0.18 for Baltimore and Beijing under inorganic-only conditions, to 1.3 for Baltimore (at an organic dry mass fraction of 0.65) and 2.5 for Beijing (organic dry mass

fraction of 0.67). ALW follows a similar trend at 70% RH as it does at 80% RH, but with lower absolute ALW levels. For the case of non-acid organics at 90% RH, increasing the organic dry mass fraction increases γ_{H+} from initial values of 0.12 and 0.20 for Baltimore and Beijing under inorganic-only conditions, to 1.2 for Baltimore (at an organic dry mass fraction of 0.79) and 0.78 for Beijing (organic dry mass fraction of 0.64). For these simulations, the ALW increases from 9.1×10^{-9} L m^{-3} to 2.4×10^{-8} L m^{-3} and from 2.1×10^{-7} L m^{-3} to 3.6×10^{-7} L m^{-3} for Baltimore and Beijing, respectively. In each case, the data plotted in Figures 1 and 2 are those that are determined not to have LLPS according to the parameterization of Bertram et al. (2011).

The plots of ALW display distinct behaviors attributable to the way in which the water content was derived for the model systems. For the organic acid simulations, the ALW was taken directly from the E-AIM Model IV output of aqueous phase water (mol m^{-3}) run with inorganic and organic acid inputs. For all non-acid organic cases, total ALW ($W_i + W_o$) was determined according to the manual AIOMFAC output fitting/polynomial fit correlation described in the methods section (Figure 1). This results in system water behavior described by polynomial fits of additional water versus organic dry mass fraction.

Effects of WSOC on Aerosol pH

The model-predicted effects of WSOC on aerosol pH are shown in Figures 2 - 5. As the dry organic mass fraction increases, ALW increases as well, since the RH and inorganics are held constant. This suggests a diluting effect, which would increase pH, in agreement with Guo et al. (2015). On the other hand, γ_{H+} also increases with increasing dry organic mass fraction, indicating that the addition of WSOC compounds increases the acidity (decreases pH).

For the case of non-acid WSOC additions (Figs. 2and 3), increasing the organic mass fraction decreases the predicted aerosol pH from the initial inorganic-only values from 1.64 to a max of 1.94 (Baltimore) and from 4.29 to a max of 4.38 (Beijing) at 80% RH. For the 70% RH simulations, the model predicted pH changes from 1.49 to a max of 1.88 for Baltimore, and from 4.10 to a max of 4.33 for Beijing. For the 90% RH case, the model predicted pH changes from 1.85 to a max of 2.09 for Baltimore, and from 4.52 to a max of 4.56 for Beijing. The transition in the pH plots are smooth, where the contour lines reflect individual levels of the factorial design and highlight the overall trend: as non-acidic WSOC is added, AIOMFAC-predicted aerosol pH increases for both the Baltimore and Beijing conditions. Since the WSOC leads to ALW uptake (diluting acidity), the increase in pH comes about due to the increase ALW having a stronger effect than the increase in γ_{H+}.

For the case of organic acids, increasing the organic mass fraction results in only slight changes in the predicted aerosol pH for Baltimore (Figure 4), but more pronounced changes for Beijing (Figure 5). At 80% RH, the predicted pH ranges from an initial (inorganic-only) value of 1.49 (Baltimore) and 4.2 (Beijing) to 1.34 and 2.6, respectively (total range = 0.4 and 1.68 pH units respectively). Similarly, there is a change from 1.33 to 1.22 (range = 0.34 pH units) for Baltimore and a change from 4.06 to 2.52 (range=1.58 pH units) for the Beijing simulations at 70% RH. Finally, there is a change from 1.75 to 1.54 (range = 0.47) for Baltimore and a change from 4.44 to 2.68 (range = 1.78) for Beijing at 90% RH. The ranges represent the total range spread from highest to lowest model-predicted pH. For Baltimore, organic acids are predicted to have only a slight effect on aerosol pH. Under the highly acidic conditions typical of the eastern U.S. (inorganic-only pH ~1), pH changes are always < 0.5 pH units, even when the dry organic aerosol mass fraction exceeds 60% (corresponding to total aerosol organic acid concentrations up

418 to 12 μg m^{-3}). This is likely due to the pH being sufficiently acidic that the organic acid
419 dissociation is largely inhibited. The undissociated organic acids still contribute ALW and affect
420 γ_{H+}, but the combined effects produce very minor modifications to pH. For Beijing, aerosol pH
421 changes are predicted to be me more substantial with the addition of organic acids, due to the
422 initially-higher aerosol pH. As organic acids are added, they can dissociate and contribute free
423 H^+. However, pH changes in excess of 1 pH unit only occur at dry organic mass fractions > 0.5.
424 Given the high inorganic aerosol concentrations in Beijing, such pH changes in excess of 1 pH
425 unit correspond to unrealistically-high aerosol organic acid mass concentrations (> 35 μg m^{-3}).
426 The relatively minor effect of organic acids on aerosol pH in Beijing is partly due to the high
427 concentrations of ammonia (Tot-NHx in Beijing = 32.8 μg m^{-3}), which also contribute to the
428 much higher "inorganics-only" pH compared to the eastern U.S. conditions.

429 The effect of organic acids on pH is closely tied to acid strength (i.e., pK_a value). Figure 6
430 shows that organic acids affect pH in the order of their pK_a values, with oxalic acid (pK_{a1} = 1.23)
431 > malonic acid (pK_{a1} = 2.83) > glutaric acid (pK_{a1} = 4.31) (Lide, 1994). The simulations with a
432 single organic acid demonstrate this effect most clearly: addition of 40 μg m^{-3} oxalic, malonic,
433 and glutaric acid produce pH changes of -1.3, -0.5, and -0.2 pH units, respectively. The pH
434 changes are all negative, indicating that the organic acids have increased particle acidity (H^+).
435 Note that although the molar amounts added are not equivalent, the observed pH changes
436 represent log-scale changes to the H^+ activity and the effect does proceed in the order of acid
437 strength.

438 The magnitudes of these observed pH changes, with the exception of the Beijing organic acids
439 case at high organic mass fractions (> 35 μg m^{-3} acids concentration) is not expected to
440 significantly alter particle conditions or lead to substantial changes in particle chemistry. For

example, ~0.5 pH unit changes should not significantly alter IEPOX uptake (Xu et al., 2015) or metal dissolution (Fang et al., 2017), two processes affected by particle acidity. An exception would be conditions where the pH is close to the point where a given species is almost equally partitioned between the gas and particle phases (*i.e.* on the center/vertical portion of the titration-style sigmoid curves). This effect is demonstrated in the work of (Guo et al., 2018b; Vasilakos et al., 2018): when the pH lays on or near the inflection point of the sigmoid curve, a change of 0.5 pH units can have significant effect on species partitioning; however, when the pH is in the flatter regions of the curve above or below the rapid transitional region, a change of 0.5 pH units will have negligible effect on partitioning, and thus particle chemistry.

Taken together, these results indicate that, despite organic mass fractions greater than 60% (dry particle mass basis), the combined effects of WSOC species on model-predicted aerosol pH is only about 0.5 pH units, maximum, with most pH changes < 0.2 pH units. This result is observed for non-acidic WSOC species and realistic concentrations of organic acids, and for simulations with a single organic compound added or for mixtures (**Table 2**). This suggests that the overall effect of WSOC on aerosol pH is quite minimal in conditions where LLPS does not occur. This finding holds only for systems in which there is no LLPS and the solvent is H_2O. For systems in which LLPS does occur, a condition expected in systems with O:C ratio of the organic material ≤ 0.5, or RH < 60% with organic:sulfate mass ratio < 1 (Bertram et al., 2011; You et al., 2013), the situation becomes more complicated. As LLPS scenarios still require equilibrium between both predominantly-aqueous and predominately-organic phases, there is both water and inorganic ions (including H^+) in the organic phase, and organics in the inorganic-rich aqueous phase (Zuend and Seinfeld, 2012; Pye et al., 2018). Thus the IUPAC definition of

pH could be applied to either phase so long as H^+ activity could be defined, necessitating an understanding of if and when LLPS occurs, and the phase for which pH is being reported.

This work stands apart from, but connects to related works. (Pye et al., 2018) specifically examined the effects of LLPS, but the present study examines a different particle regime altogether (single aqueous phase with water, inorganics, and organics); instances where LLPS were predicted to occur were excluded from the analysis for this reason.

Our findings are supported by the work of (Song et al., 2018b), who utilized E-AIM Model IV and ISORROPIA to model the same Beijing winter haze conditions, and found that addition of oxalic acid (set at 20% of the sulfate concentration) to their model in E-AIM produced reductions in pH of only 0.07 pH units. Our results are also consistent with those of (Vasilakos et al., 2018), who observed a similarly minor effect of oxalate addition on aerosol pH in the Eastern U.S., and(Nah et al., 2018) where oxalic acid/oxalate gas-particle partitioning predicted without considering organic species in the thermodynamic analysis was in reasonable agreement with measurements. Our results indicate that additions of weaker organic acids, even at higher concentrations, would have even less of an effect on pH.

A limitation of this study is that the model simulations were only run at three RH levels (70%, 80%, and 90%), with metastable conditions enforced at all times. However, aerosol particles progress through a wider RH range in the atmosphere, with concomitant effects on aerosol liquid water and phase transitions. Future work would need to expand on the RH range in order to elucidate the behavior as the system transitions from the LLPS condition to the fully mixed aqueous condition, and the contribution of changing ALW. Additionally, the use of E-AIM Model IV imposes composition limitations on the inputs (i.e., no support for Ca^{2+}, Mg^{2+}, or K^+;

485 limited support for Na^+ in the presence of NH_4^+ and Cl^-), necessitating the use of equivalent
486 cations to maintain electroneutrality in the model inputs. Combined with the use of metastable
487 calculations, there exists a potential source of error in the solution activity if these species are
488 considered and allowed to precipitate out in the thermodynamic model calculations (e.g.,
489 $CaSO_4$). As AIOMFAC relies on specific, uniquely-defined functional group interactions in the
490 composition of activity coefficients, the exchange of a non-supported cation in E-AIM for a
491 charge-equivalent cation may have effects on the output unknown to us carried through to the
492 calculation of the species activity coefficients in AIOMFAC; this is a limitation of
493 thermodynamic models that has been previously discussed (Jacobson, 1999; Kim and Seinfeld,
494 1995).

495 Another limitation of this study is consideration of only six WSOC species, despite hundreds or
496 thousands being present in atmospheric particles. This is a limitation we acknowledge, but is
497 based on the significant number of model runs given the factorial design paradigm, and the
498 decision to utilize only compounds predefined in the thermodynamic models (particularly the
499 AIOMFAC model, which allows users to create organic molecules by combining subgroups).
500 Because the compounds selected here have relatively low molecular weight (MW), is it possible
501 that higher MW compounds, such as humic-like substances (HULIS), may impart a different
502 effect. However, given the consistent results found here for both Baltimore and Beijing
503 conditions across the 70-90% RH range, and at organic dry mass fractions that range from 0 -
504 60% utilizing WSOC containing four moieties, we feel our results do represent conditions in
505 atmospheric particles. Future studies would be necessary to expand the selection of WSOC
506 compounds, and thus broaden the results reported here. Because we have forced the metastable
507 mode on our use of the models, the system mixing state becomes another potentially significant

source of error. Here we have considered only internally mixed aerosol particles without LLPS, a case that may not exist given the concentration of organic species utilized in the model study; formation of solid precipitates may occur, which has the potential to drastically alter the aqueous phase activity values. The most significant restriction of this study is the lack of observational data for comparison. Direct measurements of particle pH have so far been restricted to simple laboratory particles of specific super-micron sizes and compositions (Rindelaub et al., 2016).

4. Conclusions and Implications

In this work, the effects of WSOC on model-predicted aerosol pH were evaluated. Different inorganic datasets from Baltimore and Beijing winter haze conditions representing distinct inorganic composition regimes were first modeled in aerosol thermodynamic equilibrium models (E-AIM or ISORROPIA), then combined with six different organic species in AIOMFAC to determine the effects on aqueous-phase γ_{H+} and a_{H+}. We find that the effects of non-acid WSOC species to each of the regions has only a modest effect on aerosol pH (< 0.5 pH units, with most < 0.2 pH units). These small effects on pH were predicted even up to organic dry mass in excess of 60%. Organic acids are predicted to have a similarly small effect on pH in the eastern U.S. In Beijing, organic acids can have larger effects on pH (in excess of 2 pH units), but require stronger organic acids (pK_a values lower than the inorganic-only pH) present at high concentrations, on the same order of molar concentration as the dissociating inorganic species. The magnitude of these changes to aerosol pH are consistent with the results predicted by previous studies that considered only inorganic aerosol components combined with *a priori* knowledge of organic mass, organic water contribution, and organic species hygroscopicity (Guo et al., 2015; Bougiatioti et al., 2016).

The results of this study have important implications for the aerosol modeling community as well as for experimental studies that utilize phase partitioning data to constrain aerosol pH. Previous studies have postulated on the effect of organic species while ignoring their inclusion, or included them in order to elucidate the effects of LLPS, but this study demonstrates that in the case of single-phase systems, including these species may only contribute unnecessary complexity to the model runs. As their effects are predominantly < 0.5 pH units, it is not expected that the inclusion of organics will cause the pH of the system to reach any significant transitions unless the organic components have already driven the system to a sensitive portion of the species partitioning sigmoid curves, or aerosols in which there is significant phase separation. This work demonstrates that inclusion of large quantities of organic components does not appear to have a significant effect on model-predicted aerosol pH, consistent with the findings of (Guo et al., 2018a) and Vasilakos et al. (2018). Based on the species and concentrations of the organics studied here, future aerosol modeling studies carried out under conditions where LLPS is not occurring may be justified in the use of inorganic-only aerosol thermodynamic equilibrium models to predict aerosol pH without the direct inclusion of organic species.

Data Availability

All model inputs and outputs are available at https://knb.ecoinformatics.org/ (doi: TBD –upon acceptance).

Author Contributions

CH and MB devised the study. MB performed all modeling analyses. CH, MB, RW and AN collaborated on interpreting the results. MB prepared the manuscript, with significant contributions from CH, RW and AN.

Competing Interests

The authors declare that they have no conflict of interest.

Acknowledgements

M.A.B. and C.J.H. were supported by NSF Grant # CHE-1454763. A.N. acknowledges support from the project PyroTRACH (ERC-2016-COG) funded from H2020-EU.1.1. - Excellent Science - European Research Council (ERC), project ID 726165. R.J.W. recognizes support from the US EPA under grant 835882.

References

CRC Handbook of Chemistry and Physics, 75th ed., edited by: Lide, D. R., CRC Press, Inc., Ann Arbor, MI,

Ahrens, L., et al.: Improved characterization of gas–particle partitioning for per- and polyfluoroalkyl substances in the atmosphere using annular diffusion denuder samplers, Environmental Science & Technology, 46, 7199-7206, 10.1021/es300898s, 2012.

Battaglia, M. A., Douglas, S., and Hennigan, C. J.: Effect of the Urban Heat Island on Aerosol pH, Environmental Science & Technology, 51, 13095-13103, 10.1021/acs.est.7b02786, 2017.

Bertram, A. K., et al.: Predicting the relative humidities of liquid-liquid phase separation, efflorescence, and deliquescence of mixed particles of ammonium sulfate, organic material, and water using the organic-to-sulfate mass ratio of the particle and the oxygen-to-carbon elemental ratio of the organic component, Atmospheric Chemistry and Physics, 11, 10995-11006, 10.5194/acp-11-10995-2011, 2011.

Bikkina, S., Kawamura, K., and Miyazaki, Y.: Latitudinal distributions of atmospheric dicarboxylic acids, oxocarboxylic acids, and -dicarbonyls over the western North Pacific: Sources and formation pathways, Journal of Geophysical Research-Atmospheres, 120, 5010-5035, 10.1002/2014jd022235, 2015.

Bougiatioti, A., et al.: Particle water and pH in the eastern Mediterranean: source variability and implications for nutrient availability, Atmospheric Chemistry and Physics, 16, 4579-4591, 10.5194/acp-16-4579-2016, 2016.

Carlton, A. G., Wiedinmyer, C., and Kroll, J. H.: A review of Secondary Organic Aerosol (SOA) formation from isoprene, Atmos Chem Phys, 9, 4987-5005, 2009.

Chameides, W. L.: The Photochemistry of a Remote Marine Stratiform Cloud, Journal of Geophysical Research-Atmospheres, 89, 4739-4755, 10.1029/JD089iD03p04739, 1984.

Dallemagne, M. A., Huang, X. Y., and Eddingsaas, N. C.: Variation in pH of Model Secondary Organic Aerosol during Liquid-Liquid Phase Separation, Journal of Physical Chemistry A, 120, 2868-2876, 10.1021/acs.jpca.6b00275, 2016.

Fang, T., et al.: Highly Acidic Ambient Particles, Soluble Metals, and Oxidative Potential: A Link between Sulfate and Aerosol Toxicity, Environ Sci Technol, 51, 2611-2620, 10.1021/acs.est.6b06151, 2017.

Fountoukis, C., and Nenes, A.: ISORROPIA II: a computationally efficient thermodynamic equilibrium model for K^+-Ca^{2+}-Mg^{2+}-NH_4^+-Na^+-SO_4^{2-}-NO_3^--Cl^--H_2O aerosols, Atmos. Chem. Phys., 7, 4639-4659, 10.5194/acp-7-4639-2007, 2007.

Freedman, M. A.: Phase separation in organic aerosol, Chem Soc Rev, 46, 7694-7705, 10.1039/c6cs00783j, 2017.

595 Friese, E., and Ebel, A.: Temperature Dependent Thermodynamic Model of the System H+-
596 NH4+-Na+-SO42-NO3--Cl--H2O, J. Phys. Chem. A, 114, 11595-11631, 10.1021/jp101041j,
597 2010.

598 Guo, H., et al.: Fine-particle water and pH in the southeastern United States, Atmos Chem Phys,
599 15, 5211-5228, 10.5194/acp-15-5211-2015, 2015.

600 Guo, H., et al.: Fine particle pH and the partitioning of nitric acid during winter in the
601 northeastern United States, Journal of Geophysical Research: Atmospheres, 121, 10,355-
602 310,376, 10.1002/2016JD025311, 2016.

603 Guo, H., et al.: Fine particle pH and gas–particle phase partitioning of inorganic species in
604 Pasadena, California, during the 2010 CalNex campaign, Atmos. Chem. Phys., 17, 5703-5719,
605 10.5194/acp-17-5703-2017, 2017.

606 Guo, H., Nenes, A., and Weber, R. J.: The underappreciated role of nonvolatile cations in aerosol
607 ammonium-sulfate molar ratios, Atmos. Chem. Phys., 18, 17307-17323, 10.5194/acp-18-17307-
608 2018, 2018a.

609 Guo, H., et al.: Effectiveness of ammonia reduction on control of fine particle nitrate, Atmos.
610 Chem. Phys., 18, 12241-12256, 10.5194/acp-18-12241-2018, 2018b.

611 Gwynn, R. C., Burnett, R. T., and Thurston, G. D.: A time-series analysis of acidic particulate
612 matter and daily mortality and morbidity in the Buffalo, New York, region, Environ Health
613 Persp, 108, 125-133, Doi 10.2307/3454510, 2000.

614 Hallquist, M., et al.: The formation, properties and impact of secondary organic aerosol: current
615 and emerging issues, Atmospheric Chemistry and Physics, 9, 5155-5236, 2009.

616 Hennigan, C. J., et al.: A critical evaluation of proxy methods used to estimate the acidity of
617 atmospheric particles, Atmospheric Chemistry and Physics, 15, 2775-2790, 10.5194/acp-15-
618 2775-2015, 2015.

619 Huang, R.-J., et al.: High secondary aerosol contribution to particulate pollution during haze
620 events in China, Nature, 514, 218-222, 10.1038/nature13774, 2014.

621 Jacobson, M. Z.: Studying the effects of calcium and magnesium on size-distributed nitrate and
622 ammonium with EQUISOLV II, Atmos Environ, 33, 3635-3649, Doi 10.1016/S1352-
623 2310(99)00105-3, 1999.

624 Jia, S., et al.: Technical note: Comparison and interconversion of pH based on different standard
625 states for aerosol acidity characterization, Atmos. Chem. Phys., 18, 11125-11133, 10.5194/acp-
626 18-11125-2018, 2018.

627 Johnson, A. H., et al.: Seven Decades of Calcium Depletion in Organic Horizons of Adirondack
628 Forest Soils, Soil Science Society of America Journal, 72, 1824-1830, 10.2136/sssaj2006.0407,
629 2008.

Kanakidou, M., et al.: Past, Present, and Future Atmospheric Nitrogen Deposition, Journal of the Atmospheric Sciences, 73, 2039-2047, 10.1175/jas-d-15-0278.1, 2016.

Kawamura, K., and Bikkina, S.: A review of dicarboxylic acids and related compounds in atmospheric aerosols: Molecular distributions, sources and transformation, Atmos Res, 170, 140-160, 10.1016/j.atmosres.2015.11.018, 2016.

Keene, W. C., et al.: Aerosol pH in the marine boundary layer: A review and model evaluation, J Aerosol Sci, 29, 339-356, Doi 10.1016/S0021-8502(97)10011-8, 1998.

Keene, W. C., et al.: Closure evaluation of size-resolved aerosol pH in the New England coastal atmosphere during summer, Journal of Geophysical Research: Atmospheres, 109, D23307, 10.1029/2004jd004801, 2004.

Keppel, G.: Design and Analysis: A Researcher's Handbook, 3rd ed., Prentice-Hall, Inc., Englewood Cliffs, NJ, US, 1991.

Kim, Y. P., and Seinfeld, J. H.: Atmospheric Gas-Aerosol Equilibrium .3. Thermodynamics of Crustal Elements Ca2+, K+, and Mg2+, Aerosol Sci Tech, 22, 93-110, Doi 10.1080/02786829408959730, 1995.

Myriokefalitakis, S., et al.: Bioavailable atmospheric phosphorous supply to the global ocean: a 3-D global modeling study, Biogeosciences, 13, 6519-6543, 10.5194/bg-13-6519-2016, 2016.

Myriokefalitakis, S., et al.: Reviews and syntheses: the GESAMP atmospheric iron deposition model intercomparison study, Biogeosciences, 15, 6659-6684, 10.5194/bg-15-6659-2018, 2018.

Nah, T., et al.: Characterization of aerosol composition, aerosol acidity, and organic acid partitioning at an agriculturally intensive rural southeastern US site, Atmos. Chem. Phys., 18, 11471-11491, 10.5194/acp-18-11471-2018, 2018.

Nenes, A., et al.: Atmospheric acidification of mineral aerosols: a source of bioavailable phosphorus for the oceans, Atmos Chem Phys, 11, 6265-6272, DOI 10.5194/acp-11-6265-2011, 2011.

Peters, A., et al.: Acute health effects of exposure to high levels of air pollution in eastern Europe, Am J Epidemiol, 144, 570-581, 1996.

Pye, H. O. T., et al.: Coupling of organic and inorganic aerosol systems and the effect on gas–particle partitioning in the southeastern US, Atmos. Chem. Phys., 18, 357-370, 10.5194/acp-18-357-2018, 2018.

Rindelaub, J. D., et al.: Direct Measurement of pH in Individual Particles via Raman Microspectroscopy and Variation in Acidity with Relative Humidity, Journal of Physical Chemistry A, 120, 911-917, 10.1021/acs.jpca.5b12699, 2016.

Robinson, R. A., and Stokes, R. H.: Electrolyte solutions, 2nd revised ed., Butterworths, London, 1965.

Schindler, D. W.: Effects of acid rain on freshwater ecosystems, Science, 239, 149-157, 10.1126/science.239.4836.149, 1988.

Seinfeld, J. H., and Pandis, S. N.: Atmospheric chemistry and physics: from air pollution to climate change, 3 ed., John Wiley & Sons, Hoboken, 2016.

Song, M., et al.: Liquid-liquid phase separation in organic particles containing one and two organic species: importance of the average O: C, Atmospheric Chemistry and Physics, 18, 12075-12084, 10.5194/acp-18-12075-2018, 2018a.

Song, S., et al.: Fine-particle pH for Beijing winter haze as inferred from different thermodynamic equilibrium models, Atmos. Chem. Phys., 18, 7423-7438, 10.5194/acp-18-7423-2018, 2018b.

Spengler, J. D., et al.: Health effects of acid aerosols on North American children: Air pollution exposures, Environ Health Persp, 104, 492-499, Doi 10.2307/3432989, 1996.

Tan, T. Y., et al.: New insight into PM2.5 pollution patterns in Beijing based on one-year measurement of chemical compositions, Science of the Total Environment, 621, 734-743, 10.1016/j.scitotenv.2017.11.208, 2018.

Trebs, I., et al.: The NH4+-NO3--Cl--SO42--H2O aerosol system and its gas phase precursors at a pasture site in the Amazon Basin: how relevant are mineral cations and soluble organic acids?, Journal of Geophysical Research: Atmospheres, 110, 10.1029/2004jd005478, 2005.

Vasilakos, P., Russell, A., Weber, R., and Nenes, A.: Understanding nitrate formation in a world with less sulfate, Atmos. Chem. Phys., 18, 12765-12775, 10.5194/acp-18-12765-2018, 2018.

Wang, G., et al.: Persistent sulfate formation from London Fog to Chinese haze, Proceedings of the National Academy of Sciences, 10.1073/pnas.1616540113, 2016.

Weber, R. J., Guo, H., Russell, A. G., and Nenes, A.: High aerosol acidity despite declining atmospheric sulfate concentrations over the past 15 years, Nature Geoscience, 9, 282-285, 10.1038/ngeo2665, 2016.

Wexler, A. S., and Clegg, S. L.: Atmospheric aerosol models for systems including the ions H^+, NH_4^+, Na^+, SO_4^{2-}, NO_3^-,Cl^-, Br^-, and H_2O, J Geophys Res-Atmos, 107, Artn 4207

Doi 10.1029/2001jd000451, 2002.

Xu, L., et al.: Effects of anthropogenic emissions on aerosol formation from isoprene and monoterpenes in the southeastern United States, Proceedings of the National Academy of Sciences, 112, 37-42, 10.1073/pnas.1417609112, 2015.

Yatavelli, R. L. N., et al.: Estimating the contribution of organic acids to northern hemispheric continental organic aerosol, Geophysical Research Letters, 42, 6084-6090, 10.1002/2015gl064650, 2015.

You, Y., Renbaum-Wolff, L., and Bertram, A. K.: Liquid-liquid phase separation in particles containing organics mixed with ammonium sulfate, ammonium bisulfate, ammonium nitrate or sodium chloride, Atmos. Chem. Phys., 13, 11723-11734, 10.5194/acp-13-11723-2013, 2013.

Zhou, W., et al.: Characterization and source apportionment of organic aerosol at 260 m on a meteorological tower in Beijing, China, Atmospheric Chemistry and Physics, 18, 3951-3968, 10.5194/acp-18-3951-2018, 2018.

Zuend, A., Marcolli, C., Luo, B. P., and Peter, T.: A thermodynamic model of mixed organic-inorganic aerosols to predict activity coefficients, Atmospheric Chemistry and Physics, 8, 4559-4593, 2008.

Zuend, A., et al.: New and extended parameterization of the thermodynamic model AIOMFAC: calculation of activity coefficients for organic-inorganic mixtures containing carboxyl, hydroxyl, carbonyl, ether, ester, alkenyl, alkyl, and aromatic functional groups, Atmos. Chem. Phys., 11, 9155-9206, 10.5194/acp-11-9155-2011, 2011.

Zuend, A., and Seinfeld, J. H.: Modeling the gas-particle partitioning of secondary organic aerosol: the importance of liquid-liquid phase separation, Atmospheric Chemistry and Physics, 12, 3857-3882, 10.5194/acp-12-3857-2012, 2012.

Figures:

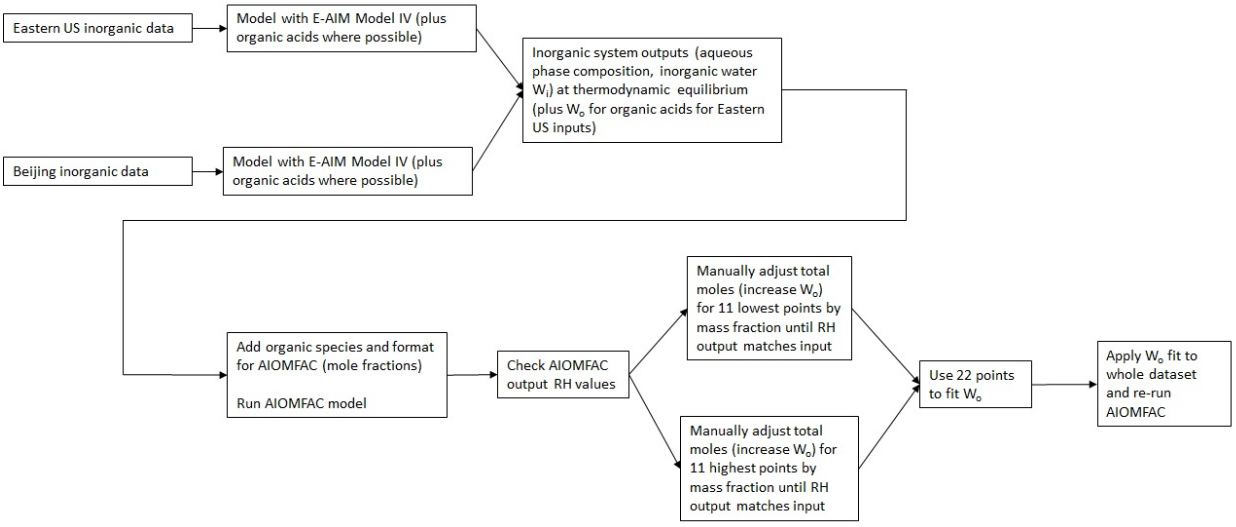

Figure 1: Flow diagram for adjusting total moles in the organic/inorganic mixed system inputs for the AIOMFAC model. Total moles were adjusted (representing increased W_o) of the first 11 and last 11 model points until the AIOMFAC-output RH was within 5% of the fixed model input value (70%, 80%, or 90%). These 22 points were then used to fit a polynomial function to correct the total system moles for the remaining 1309 data points.

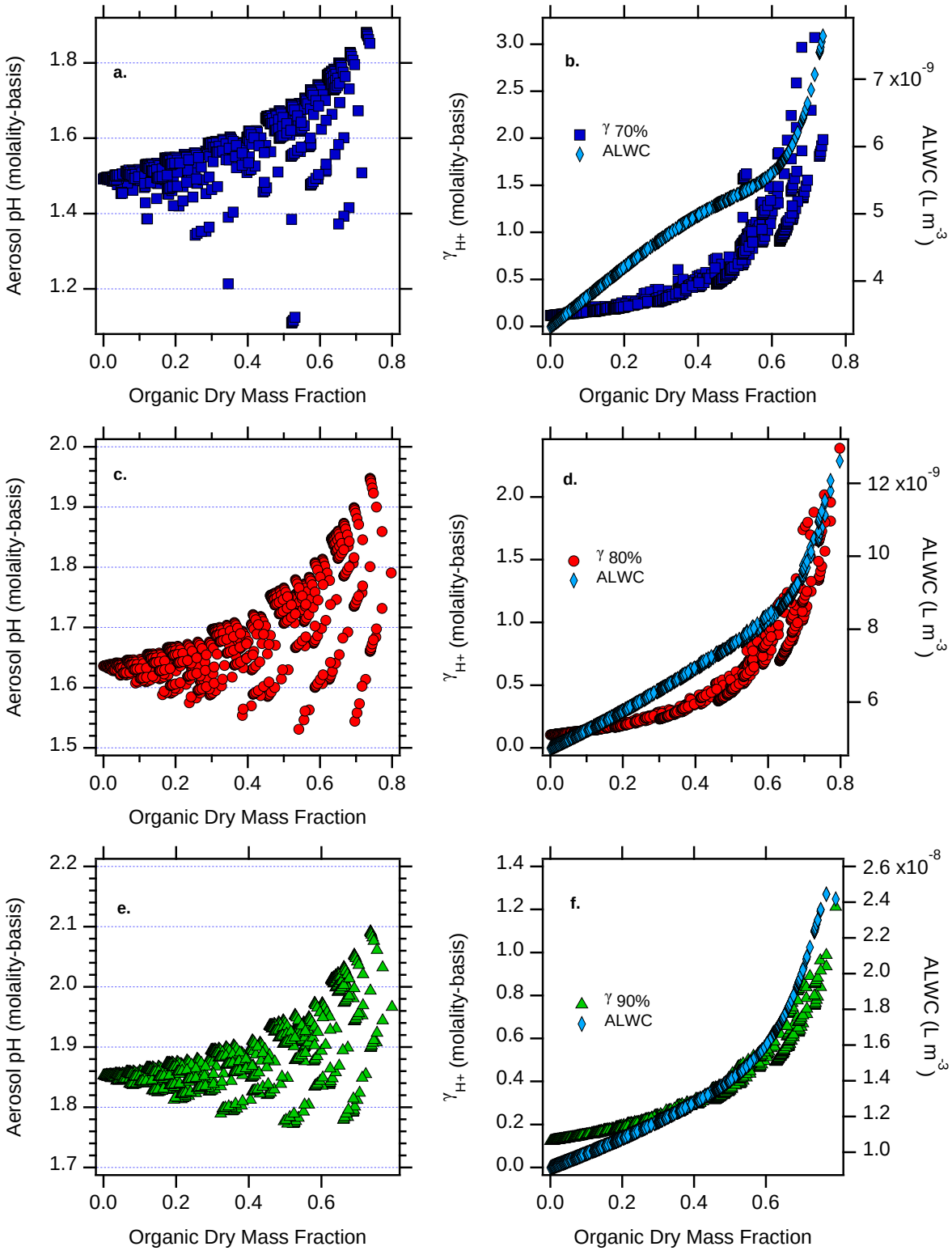

Figure 2: AIOMFAC-modeled aerosol pH (molality basis) versus organic dry mass fraction with the factorial addition of non-acid organic species and AIOMFAC-modeled γ_{H^+} (molality

basis) and aerosol liquid water (ALW, polynomial fit to AIOMFAC output) versus organic dry mass fraction (right panel) for Baltimore at a) and b)70% RH, c) and d) 80% RH, and e) and f) 90% RH.

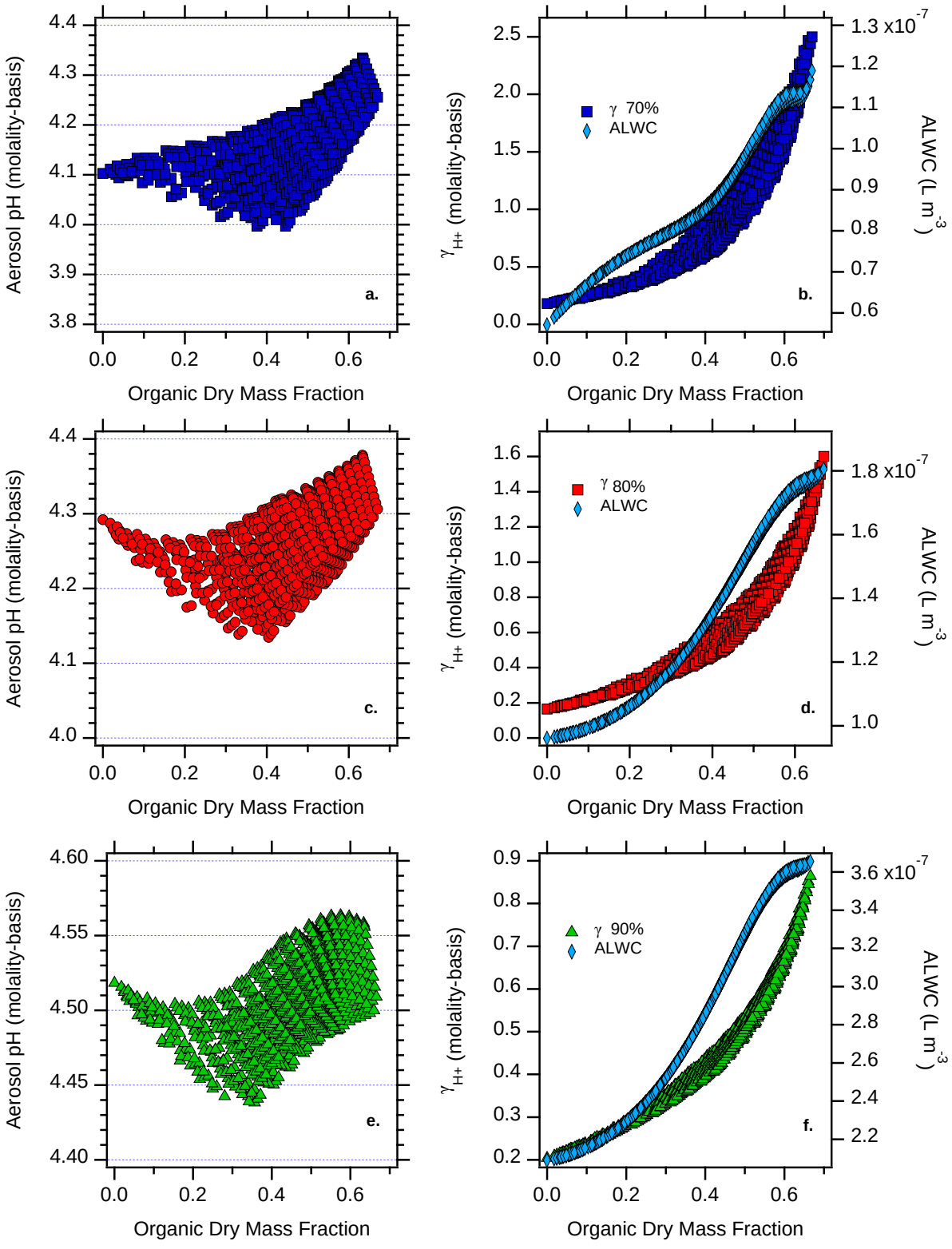
Aerosol pH (molality-basis)
Organic Dry Mass Fraction
a.
γ 70%
ALWC
γH+ (molality-basis)
ALWC (L m-3)
1.3 x10-7
b.
γ 80%
1.8 x10-7
c.
d.
γ 90%
3.6 x10-7
e.
f.

Figure 3: AIOMFAC-modeled aerosol pH (molality basis) versus organic dry mass fraction with the factorial addition of non-acid organic species and AIOMFAC-modeled γ_{H^+} (molality basis) and aerosol liquid water (ALW, polynomial fit to AIOMFAC output) versus organic dry mass fraction (right panel) for Beijing at a) and b) 70% RH, c) and d) 80% RH, and e) and f) 90% RH.

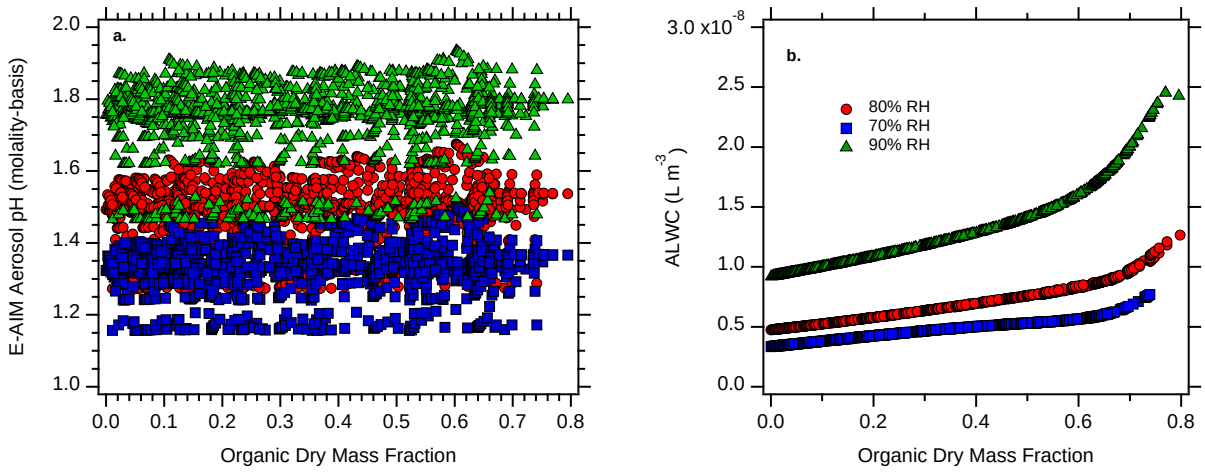

Figure 4: E-AIM-modeled (a) aerosol pH (molality basis) and (b) ALW at 70% (blue), 80% (red), and 90% RH (green) levels for the Baltimore simulations with organic acids.

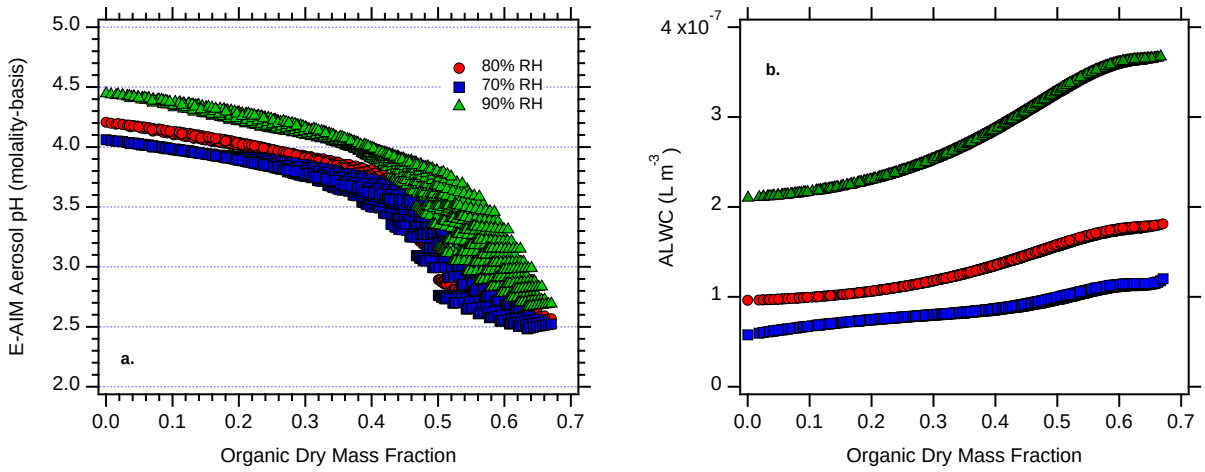

Figure 5: E-AIM-modeled (a) aerosol pH (molality basis) and (b) ALW at 70% (blue), 80% (red), and 90% RH (green) levels for the Beijing simulations with organic acids.

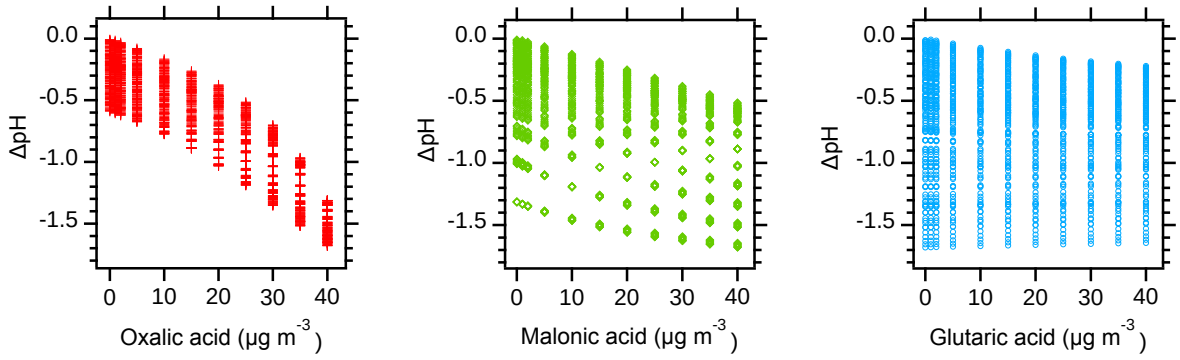

Figure 6: ΔpH vs. discrete organic acid levels for the organic acid pH calculations carried out in E-AIM for Baltimore and Beijing. ΔpH represents the difference between the initial 'inorganic-only' pH prediction and all other model evaluations where organic acids were present.

Table 1: Summary of model runs performed for the study. Inorganic composition is invariant and taken from the sources provided. Organic components were added in factorial fashion.

Location	Inorganic Data	Inorganic Equilibrium Model	Organic components	# of Points
Baltimore	Battaglia et al. 2017	E-AIM Model IV	Organic Acids	1331
Baltimore	Battaglia et al. 2017	E-AIM Model IV	Non-acid organics	1331
Beijing	Guo et al. 2018b	ISORROPIA 2.3 E-AIM Model IV	Organic acids	1331
Beijing	Guo et al. 2018b	ISORROPIA 2.3 E-AIM Model IV	Non-acid organics	1331

Table 2: Whole species inorganic inputs used in AIOMFAC modeling at 70%, 80%, or 90% RH. Inorganic equilibrium outputs were used to assign anions to cations to form whole species, represented here. Entries marked with a dash represent components not used for the given location as a result of anion or cation not being present in the composition data (species not measured).

Component	Baltimore Conc. (mol m^{-3}) 70% RH	Baltimore Conc. (mol m^{-3}) 80% RH	Baltimore Conc. (mol m^{-3}) 90% RH	Beijing Conc. (mol m^{-3}) 70% RH	Beijing Conc. (mol m^{-3}) 80% RH	Beijing Conc. (mol m^{-3}) 90% RH
H_2SO_4	1.488×10^{-10}	2.418×10^{-10}	3.326×10^{-10}	3.13×10^{-12}	6.273×10^{-12}	1.010×10^{-11}
NH_4HSO_4	3.460×10^{-9}	2.612×10^{-9}	1.899×10^{-9}	4.057×10^{-11}	3.173×10^{-11}	2.307×10^{-11}
$(NH_4)_2SO_4$	2.395×10^{-8}	2.318×10^{-8}	2.425×10^{-8}	2.710×10^{-7}	2.710×10^{-7}	2.710×10^{-7}
$NaNO_3$	6.425×10^{-11}	1.207×10^{-10}	3.573×10^{-10}	-	-	-
Na_2SO_4	1.403×10^{-9}	1.375×10^{-9}	1.257×10^{-9}	-	-	-
NH_4Cl	-	-	-	4.793×10^{-8}	4.797×10^{-8}	4.799×10^{-8}
NH_4NO_3	-	-	-	4.189×10^{-7}	4.189×10^{-7}	4.190×10^{-7}